Clim. Past Discuss., 11, 831–872, 2015
www.clim-past-discuss.net/11/831/2015/
doi:10.5194/cpd-11-831-2015

Climate of the Past Discussions
Open Access

Glacial–interglacial shifts in global and regional precipitation $\delta^{18}O$

S. Jasechko[1,2], A. Lechler[3], F. S. R. Pausata[4], P. J. Fawcett[1], T. Gleeson[5], D. I. Cendón[6], J. Galewsky[1], A. N. LeGrande[7], C. Risi[8], Z. D. Sharp[1], J. M. Welker[9], M. Werner[10], and K. Yoshimura[11]

[1]Department of Earth and Planetary Sciences, University of New Mexico, Albuquerque, New Mexico, USA
[2]Department of Geography, University of Calgary, Calgary, Alberta, Canada
[3]Department of Geosciences, Pacific Lutheran University, Tacoma, USA
[4]Department of Meteorology and Bolin Center for Climate Research, Stockholm University, Stockholm, Sweden
[5]Department of Civil Engineering, University of Victoria, Victoria, Canada
[6]Australian Nuclear Science and Technology Organisation, Sydney, Australia
[7]NASA Goddard Institute for Space Studies, New York, USA
[8]Laboratoire de Météorologie Dynamique, IPSL, UPMC, CNRS, Paris, France
[9]Department of Biological Sciences, University of Alaska Anchorage, Anchorage, Alaska, USA
[10]Alfred Wegener Institute, Helmholtz Centre for Polar and Marine Research, Bremerhaven, Germany
[11]Atmosphere and Ocean Research Institute, University of Tokyo, Kashiwa, Japan

Received: 28 February 2015 – Accepted: 5 March 2015 – Published: 27 March 2015

Correspondence to: S. Jasechko (sjasechk@ucalgary.ca)

Published by Copernicus Publications on behalf of the European Geosciences Union.

CPD
11, 831–872, 2015

Abstract

Previous analyses of past climate changes have often been based on site-specific isotope records from speleothems, ice cores, sediments and groundwaters. However, in most studies these dispersed records have not been integrated and synthesized in a comprehensive manner to explore the spatial patterns of precipitation isotope changes from the last ice age to more recent times. Here we synthesize 88 globally-distributed groundwater, cave calcite, and ice core isotope records spanning the last ice age to the late-Holocene. Our data-driven review shows that reconstructed precipitation δ^{18}O changes from the last ice age to the late-Holocene range from −7.1 ‰ (ice age δ^{18}O < late-Holocene δ^{18}O) to +1.8 ‰ (ice age δ^{18}O > late-Holocene δ^{18}O) with wide regional variability. The majority (75 %) of reconstructions have lower ice age δ^{18}O values than late-Holocene δ^{18}O values. High-magnitude, negative glacial–interglacial precipitation δ^{18}O shifts (ice age δ^{18}O < late-Holocene δ^{18}O by more than 3 ‰) are common at high latitudes, high altitudes and continental interiors. Conversely, lower-magnitude, positive glacial–interglacial precipitation δ^{18}O shifts (ice age δ^{18}O > late-Holocene δ^{18}O by less than 2 ‰) are most common along subtropical coasts. Broad, global patterns of glacial–interglacial precipitation δ^{18}O shifts are consistent with stronger-than-modern isotopic distillation of air masses during the last ice age, likely impacted by larger global temperature differences between the tropics and the poles. Further, to complement our synthesis of proxy-record precipitation δ^{18}O, we compiled isotope enabled general circulation model simulations of recent and last glacial maximum climate states. Simulated precipitation δ^{18}O from five general circulation models show better inter-model and model-observation agreement in the sign of δ^{18}O changes from the last ice age to present day in temperate and polar regions than in the tropics. Further model precipitation δ^{18}O research is needed to better understand impacts of inter-model spread in simulated precipitation fluxes and parameterizations of convective rainout, seawater δ^{18}O and glacial topography on simulated precipitation δ^{18}O. Future paleo-precipitation proxy record δ^{18}O research

CPD
11, 831–872, 2015

can use new global maps of glacial $\delta^{18}O$ reconstructions to target and prioritize regional investigations of past climate states.

1 Introduction

Reconstructed isotope compositions of Pleistocene precipitation preserved in groundwaters, cave calcite, glacial ice, ground ice and lake sediments have been used to better understand past climate changes for more than a half century (e.g., Münnich, 1957; Thatcher et al., 1961; Münnich et al., 1967; Pearson and White, 1967; Tamers, 1967; Gat et al., 1969). Each type of isotopic proxy record is distinguished by its temporal resolution, preservation of one or both $^{18}O/^{16}O$ and $^{2}H/^{1}H$ ratios, and frequency of records on land surface. For example, groundwater records contain both $^{18}O/^{16}O$ and $^{2}H/^{1}H$ ratios with widespread global occurrence, but have a coarser temporal resolution than other paleoclimate proxies (Rozanski et al., 1985; Edmunds and Milne, 2001; Edmunds, 2009; Corcho Alvarado et al., 2010; Jiráková et al., 2011). Speleothem records, in contrast, have high temporal resolution but usually only report calcite $^{18}O/^{16}O$ ratios (without fluid inclusion $^{2}H/^{1}H$ data) and are less common than groundwater records (e.g., Harmon et al., 1978, 1979). Pleistocene glacier- and ground-ice records have high temporal resolution, can be analyzed for $^{18}O/^{16}O$ and $^{2}H/^{1}H$ ratios, but are rare on non-polar lands (Dansgaard et al., 1982; Thompson et al., 1989, 1995, 1997, 1998). Lake sediment records can have high temporal resolution, can preserve $^{18}O/^{16}O$ and $^{2}H/^{1}H$ ratios and are available for a multitude of globally-distributed locations (e.g., Edwards et al., 1989; Eawag et al., 1992; Menking et al., 1997; Wolfe et al., 2000; Anderson et al., 2001; Beuning et al., 2002; Sachse et al., 2004; Morley et al., 2005; Tierney et al., 2008). However, some lake water proxy isotope records may be impacted by paleo-lake evaporative isotope effects that obscure the primary meteoric water signal and mask paleo-precipitation isotope compositions (e.g., lake sediment calcite, diatom silica; Leng and Marshall, 2004).

CPD
11, 831–872, 2015

This study focuses primarily upon groundwater isotope records due to the relative density of groundwater records in the published literature in comparison to the more limited number of published isotopic records from speleothems and ice cores (compilations by Pedro et al., 2011; Stenni et al., 2011; Clark et al., 2012; Shah et al., 2013; Caley et al., 2014a). There exist roughly twice as many groundwater reconstructions of ice age precipitation $\delta^{18}O$ ($n = 61$) as the combined total of speleothem and ice core precipitation $\delta^{18}O$ records spanning the last ice age and late-Holocene time periods ($n = 27$; where $\delta^{18}O = (^{18}O/^{16}O_{sample})/(^{18}O/^{16}O_{standard\ mean\ ocean\ water} - 1) \cdot 1000$). A recent global synthesis of paired precipitation-groundwater isotopic data demonstrated that modern annual amount-weighted precipitation and local, modern groundwater recharge isotope compositions follow systematic relationships with some bias toward winter and wet-season precipitation (Jasechko et al., 2014). Systematic rainfall-recharge relationships shown by Jasechko et al. (2014) support our primary assumption in this study that groundwater isotope compositions closely reflect meteoric water. Because groundwater records can only identify climate change occurring over thousands of years due to hydrodynamic dispersion during multi-millennial residence times (e.g., Davison and Airey, 1982; Stute and Deak, 1989), we limit the focus of this study to meteoric water isotope composition changes from the last ice age to the late-Holocene. The last ice age time period is defined as 19 500 to ~ 50 000 years before present, defined using the end of the last glacial maximum as the more recent age limit (19 500 years before present; Clark et al., 2009), and the approximate maximum age of groundwater that can be identified by ^{14}C dating as an approximate upper age limit (i.e., groundwater ages more recent than ~ 50 000 years). We adopt a definition of the late-Holocene as occurring within the last 5000 years following Thompson et al. (2006). Other work proposes the late-Holocene be defined as within the last 4200 years (Walker et al., 2012), which is consistent with the 5000 years before present definition (Thompson et al., 2006) within the practical uncertainty of ^{14}C-based groundwater ages (± ~ 10^3 years). Further, although precipitation isotope

CPD
11, 831–872, 2015

compositions have varied over the late-Holocene, groundwater mixing integrates this variability, prohibiting paleoclimate interpretation at finer temporal resolutions.

Pleistocene-to-Holocene changes in precipitation isotope compositions provide important insights into conditions and processes of the past. Perhaps the two best-constrained global-in-scale differences between the last ice age and the late-Holocene are changes to oceanic and atmospheric temperatures (MARGO Members, 2009; Shakun and Carlson, 2010; Annan and Hargreaves, 2013), and changes to seawater $\delta^{18}O$ (Emiliani, 1955; Dansgaard and Tauber, 1969; Schrag et al., 1996, 2002). Atmospheric temperatures have increased by a global average of $\sim 4\,^{\circ}C$ since the last glacial maximum, with greatest warming at the poles and more modest warming at lower latitudes (Fig. S1 in the Supplement; e.g., Shakun and Carlson, 2010; Annan and Hargreaves, 2013). Seawater $\delta^{18}O$ during the last glacial maximum was 1.0 ± 0.1 ‰ higher than the modern ocean, as constrained by paleo-ocean water samples collected from pore waters trapped within sea floor sediments (Schrag et al., 2002).

Other studies have proposed other interpretations for reconstructed changes to precipitation isotope compositions of ice age and modern day precipitation. Records of past changes to precipitation $\delta^{18}O$ have been used as a proxy for regional land surface and atmospheric temperature (e.g., Rozanski, 1985; Nikolayev and Mikhalev, 1999; Johnsen et al., 2001; Grasby and Chen, 2005; Akouvi et al., 2008; Bakari et al., 2011), however, $\delta^{18}O$-based paleotemperatures can be complicated by past changes to a variety of other processes controlling precipitation $\delta^{18}O$, including moisture sources, upwind rainout, transport pathways, moisture recycling and in-cloud processes (Ciais and Jouzel, 1994; Masson-Delmotte et al., 2005; Sjostrom and Welker, 2009). Process-based explanations for observed meteoric water $\delta^{18}O$ variations in proxy records include changes to hurricane intensity (e.g., Plummer et al., 1993), large-scale atmospheric circulation (e.g., Rozanski et al., 1985; Weyhenmeyer et al., 2000; McDermott et al., 2001; Pausata et al., 2009; Asmerom et al., 2010), aridity (e.g., Wagner et al., 2010), monsoon strength (e.g., Denniston et al., 2000; Lachniet et al., 2004; Liu et al., 2007; Pausata et al., 2011a), local seawater $\delta^{18}O$

CPD
11, 831–872, 2015

(Wood et al., 2003; Feng et al., 2014), precipitation seasonality (e.g., Fawcett et al., 1997; Werner et al., 2000; Cruz et al., 2005), moisture provenance (e.g., Sjostrom and Welker, 2009; Lewis et al., 2010), storm tracks, climate oscillation modes (e.g., North Atlantic oscillation), moisture recycling (e.g., Winnick et al., 2013, 2014; Liu et al., 2014a, b) and groundwater flow path architecture (Purdy et al., 1996; Stewart et al., 2004; Morrissey et al., 2010). While unraveling these mechanisms and delineating the primary and secondary processes can be rather challenging, the use of climate models in combination with robust and extensive precipitation isotope data can resolve many of these complexities with meaningful interpretations and insight.

The objective of this study is to analyze spatial patterns of reconstructed precipitation δ^{18}O changes since the last ice age from published groundwater, ground ice, glacial ice and cave calcite records, and to compare these observations with output from five state-of-the-art isotope-enabled general circulation model simulations of last glacial maximum and more recent climate conditions. Synthesizing paleowater δ^{18}O records provides an important constraint for isotope-enabled general circulation model simulations of glacial meteorology and hydrology (Jouzel et al., 2000). We combine a new global compilation of ice age groundwater and ground ice isotope data ($n = 61$) with existing compilations of speleothem ($n = 15$; Shah et al., 2013) and ice core ($n = 11$; Pedro et al., 2011; Stenni et al., 2011; Clark et al., 2012; Caley et al., 2014a) isotope data. This compilation of ice age groundwater isotope compositions builds from earlier reviews of European and African ice age groundwater isotope compositions (Rozanski, 1985; Edmunds and Milne, 2001; Edmunds, 2009; Négrel and Petelet-Giraud, 2011; Jiráková et al., 2011).

2 Dataset and methods

In order to examine spatial patterns of change to meteoric water δ^{18}O values we compiled δ^{18}O, δ^{2}H, δ^{13}C and ^{14}C data from 1713 groundwater samples collected from 61 aquifer systems reported in 75 publications (Fig. 1). δ^{13}C, ^{3}H

CPD
11, 831–872, 2015

and ^{14}C data were used to calculate ^{14}C-based modelled groundwater ages (details within Supporting Information). Changes to precipitation $\delta^{18}O$ values over time were determined by comparing groundwater isotope compositions of the late-Holocene ($\delta^{18}O_{\text{late-Holocene}}$ defined here as less than 5000 years before present; Thompson et al., 2006) and the latter half of the last ice age ($\delta^{18}O_{\text{ice age}}$: 19 500 to ~ 50 000 years before present). We acknowledge that these two relatively long time intervals – necessarily long in order to examine groundwater isotope records – integrate precipitation $\delta^{18}O$ variability over the course of each time interval. The late-Holocene time interval integrates known precipitation $\delta^{18}O$ variability, and the "last ice age" time interval could incorporate precipitation occurring during Marine Isotope Stage 3 for groundwater records and multiple records likely incorporate groundwater preceding the last glacial maximum.

Proxy-based meteoric water $\delta^{18}O$ changes from the last ice age to the late-Holocene are described herein as *reconstructed* $\Delta^{18}O_{\text{ice age}}$, where reconstructed $\Delta^{18}O_{\text{ice age}} = \delta^{18}O_{\text{ice age}} - \delta^{18}O_{\text{late-Holocene}}$. A minimum groundwater age of 19 500 years before present was used to define the last ice age to remain consistent with the timing of the last glacial maximum (see Clark et al., 2009). Samples having a deuterium excess of less than zero (deuterium excess = $\delta^{2}H - 8 \cdot \delta^{18}O$; Dansgaard, 1964) and falling along regionally-characteristic evaporation $\delta^{2}H/\delta^{18}O$ slopes (Gibson et al., 2008) were removed from the analysis to avoid including groundwater samples impacted by partial evaporation. Further, studies reporting saltwater intrusion were avoided on the basis of groundwater $\delta^{18}O$ and salinities showing evidence of seawater mixing (e.g., Schiavo et al., 2009; Hamouda et al., 2011; Han et al., 2011; Wang and Jiao, 2012; Currell et al., 2013). The 61 compiled groundwater reconstructed $\Delta^{18}O_{\text{ice age}}$ values are unevenly distributed among western Europe ($n = 10$), eastern Europe and the Middle-East ($n = 12$), Africa ($n = 18$), southeastern Asia ($n = 6$), Australia, Oceania and the Malay Archipelago ($n = 3$), South America ($n = 2$), temperate and subtropical North America ($n = 8$) and the High Arctic ($n = 2$, ground ice records). Half the compiled

CPD
11, 831–872, 2015

groundwater records are located in the tropics or subtropics (that is, within 35° of the equator) and half are located in the extra-tropics.

Speleothem and ice core isotope proxy records were also compiled. Lacustrine sediment $\delta^{18}O$ records are not considered in this study because these records may preserve meteoric waters impacted by evaporative isotope effects. Speleothem and ice core reconstructed $\Delta^{18}O_{ice\ age}$ values were calculated by subtracting average $\delta^{18}O$ values for each of the two time intervals defined for the groundwater records: the late-Holocene (< 5000 years before present) and last ice age (19 500–50 000 years before present). This step effectively lowered the temporal resolution of speleothem and ice core precipitation isotope records to be consistent with the temporal resolution of the groundwater records. A correction factor was applied to speleothem $\delta^{18}O$ values to account for different H_2O-$CaCO_3$ isotopic fractionation factors during the last ice age and the late-Holocene imparted by the different land surface temperatures during each time period (details presented within the Supplement).

Simulated $\Delta^{18}O_{ice\ age}$ values were compiled from five isotope-enabled general circulation models (simulated $\Delta^{18}O_{ice\ age} = \delta^{18}O_{last\ glacial\ maximum} - \delta^{18}O_{pre\text{-}industrial}$): CAM3iso (e.g., Noone and Sturm, 2010; Pausata et al., 2011a), ECHAM5-wiso (e.g., Werner et al., 2011), GISSE2-R (e.g., Schmidt et al., 2014; LeGrande and Schmidt, 2008, 2009), IsoGSM (e.g., Yoshimura et al., 2003) and LMDZ4 (e.g., Risi et al., 2010a). ECHAM5-wiso and IsoGSM outputs are for modern climate rather than pre-industrial conditions, however, the difference between the isotope composition of pre-industrial and modern climate are expectedly small compared to glacial–interglacial shifts. An offset factor was applied to simulated mean seawater $\delta^{18}O$ in all five models (Table S1 in the Supplement) to account for known glacial–interglacial changes to seawater $\delta^{18}O$ (Emiliani, 1955; Dansgaard and Tauber, 1969; Schrag et al., 1996, 2002). Possible spatial differences in seawater $\delta^{18}O$ changes from the last glacial maximum to the pre-industrial time period are not incorporated into forced simulations (CAM3iso, ECHAM5-wiso, GISSE2-R, LMDZ4) but are simulated by the coupled ocean–atmosphere simulation of GISSE2-R (Table S1). In general, these models were

CPD
11, 831–872, 2015

the versions submitted to the CMIP5 archive and participated in PMIP3. Notable exceptions include IsoGSM using different boundary conditions (Yoshimura et al., 2008), ECHAM5 not participating in CMIP5, and CAM3iso not participating in PMIP3. The five models span a range of spatio-temporal resolutions and isotopic/atmospheric parameterizations described in detail in the above references. A selection of the inter-model similarities and differences are summarized in Table S1 (Supplement).

For clarity, data-based $\Delta^{18}O_{ice\ age}$ values from groundwater, speleothems, ground ice and ice cores are referred to herein as *reconstructed* $\Delta^{18}O_{ice\ age}$, whereas simulated precipitation isotope compositions from general circulation models are referred to as *simulated* $\Delta^{18}O_{ice\ age}$. We acknowledge that the general circulation models explicitly analyze the last glacial maximum and the pre-industrial climate conditions (i.e., simulated $\Delta^{18}O_{ice\ age} = \delta^{18}O_{last\ glacial\ maximum} - \delta^{18}O_{pre\text{-}industrial}$), whereas proxy record reconstructions of $\Delta^{18}O_{ice\ age}$ integrate hydroclimatology over multi-millennial time scales that are different from the model simulations (i.e., reconstructed $\Delta^{18}O_{ice\ age} = \delta^{18}O_{ice\ age} - \delta^{18}O_{late\text{-}Holocene}$).

3 Results and discussion

3.1 Reconstructed $\Delta^{18}O_{ice\ age}$ values

Reconstructed groundwater ($n = 61$), speleothem ($n = 15$) and ice core ($n = 12$) $\Delta^{18}O_{ice\ age}$ values are presented in Fig. 1 (references presented in the Supplement). Reconstructed $\Delta^{18}O_{ice\ age}$ values range from −7.1 ‰ (i.e., $\delta^{18}O_{ice\ age} < \delta^{18}O_{late\text{-}Holocene}$) to +1.8 ‰ (i.e., $\delta^{18}O_{ice\ age} > \delta^{18}O_{late\text{-}Holocene}$). Three-quarters of compiled records have negative reconstructed $\Delta^{18}O_{ice\ age}$ values and one-quarter of compiled records have positive reconstructed $\Delta^{18}O_{ice\ age}$ values. More than 80 % of reconstructed $\Delta^{18}O_{ice\ age}$ values of greater than zero are located in the within 35° of

CPD
11, 831–872, 2015

the equator and within 400 km of the nearest coastline (e.g., Bangladesh $\Delta^{18}O_{ice\ age}$ of +1.6 ‰, less than 300 km from the coast; Figs. 1 and 2; Fig. S2). In comparison, negative reconstructed $\Delta^{18}O_{ice\ age}$ values are found in both coastal regions and farther inland. Negative reconstructed $\Delta^{18}O_{ice\ age}$ values of the greatest magnitude are located at high latitudes (e.g., northwestern Canada, latitude 64°: $\Delta^{18}O_{ice\ age}$ of −5.5 ‰ ; northern Russia latitude 72°: −5.5 ‰) and far from coastlines (e.g., Hungary: −3.7 ‰, ∼ 500 km from Atlantic Ocean; Peru: −6.5 ‰, ∼ 2000 km from Atlantic Ocean, the modern moisture source to Peru, Garreaud et al., 2009). Greenland and Antarctic ice cores have negative reconstructed $\Delta^{18}O_{ice\ age}$ values that are of greater magnitude than non-polar reconstructed $\Delta^{18}O_{ice\ age}$ values (Antarctic and Greenland $\Delta^{18}O_{ice\ age}$ values range from −3.6 to −7.1 ‰ ; Fig. 2).

Reconstructed $\Delta^{18}O_{ice\ age}$ values synthesized in this study generally show that tropical $\Delta^{18}O_{ice\ age}$ values are closer to 0 ‰ (i.e., no change) than high latitude, continental regions that generally have high magnitude, negative reconstructed $\Delta^{18}O_{ice\ age}$ values. High magnitude, negative reconstructed $\Delta^{18}O_{ice\ age}$ values are most common where present day precipitation $\delta^{18}O$ values are at a minimum (e.g., Bowen and Wilkinson, 2002). This broad spatial pattern is consistent with the non-linear isotopic distillation of air masses undergoing progressive rainout (i.e., Rayleigh distillation). Because seawater $\delta^{18}O$ values were ∼ 1 ‰ higher-than-modern during the last ice age (Schrag et al., 1996, 2002), our finding that the majority of reconstructed $\Delta^{18}O_{ice\ age}$ values are negative suggests that isotopic distillation of air masses was greater during the last ice age than under present climate. This finding is consistent with land surface temperature reconstructions that show larger glacial-to-modern changes to land temperatures at high latitude and continental settings (Fig. S1; Annan and Hargreaves, 2013).

CPD
11, 831–872, 2015

3.2 Simulated $\Delta^{18}O_{ice\ age}$ values

Simulated precipitation $\Delta^{18}O_{ice\ age}$ values from five general circulation models are presented in Fig. 3. At least four of the five models agree on the sign of simulated $\Delta^{18}O_{ice\ age}$ values for 68.8 % of grid cells covering Earth's surface (68.7 % of ocean areas and 68.9 % of over land areas; multi-model calculation completed using 3 of 4 models as a threshold at high-latitudes where IsoGSM data was not available). Simulated $\Delta^{18}O_{ice\ age}$ values are consistently negative over the North Atlantic Ocean and the Fennoscandian and Laurentide ice sheets and consistently positive over most of the tropical oceans, whereas low agreement is found over tropical land surfaces. The negative simulated $\Delta^{18}O_{ice\ age}$ values over the Northern Hemisphere ice sheets and North Atlantic are likely driven by the difference in topography and sea ice cover, respectively, between the last ice age and pre-industrial climate. The glacial–interglacial change in ice sheet topography and sea ice cover impacted surface temperatures. Surface temperatures were more than ~ 20 °C cooler over most of present-day Canada during the last ice age and this temperature shift is likely to impact simulated $\Delta^{18}O_{ice\ age}$ values (Fig. S1).

A comparison of simulated $\Delta^{18}O_{ice\ age}$ values over tropical Africa, South America and Oceania shows inter-model disagreement (Fig. 3). Different tropical simulated $\Delta^{18}O_{ice\ age}$ values amongst the models reflect the different isotopic parameterizations, inter-model spread in simulated precipitation fluxes, glacial–interglacial shifts in seawater $\delta^{18}O$ (inter-model seawater $\delta^{18}O_{ice\ age}$ minus seawater $\delta^{18}O_{pre\text{-}industrial}$ ranges from +0.7 to +1.1 ‰) and seawater $\delta^{18}O$ heterogeneity used in each model. Inter-model spread in simulated $\Delta^{18}O_{ice\ age}$ values in some regions highlights the importance of this global synthesis of proxy record reconstructed $\Delta^{18}O_{ice\ age}$ values as a constraint for climate model simulated $\Delta^{18}O_{ice\ age}$ values. Another potential source for the model disagreement is introduced by the different ice-sheet topography used in each model. CAM3Iso, IsoGSM and LMDZ4 have used Ice 5G (Peltier, 1994)

CPD
11, 831–872, 2015

as advised for PMIP2 (Braconnot et al., 2007), whereas the GISSE2 replaces Ice 5G Laurentide ice with that of Licciardi et al. (1999) and ECHAM5-wiso uses ice topography from PMIP3 (Braconnot et al., 2007, 2012; PMIP3 follows ice sheet topography blended from multiple ice sheet reconstructions; e.g., Argus and Peltier, 2010; Toscano et al., 2011). Glacial topography is an important driver of simulated temperature, precipitation and atmospheric circulation at the Last Glacial Maximum (e.g., Justino et al., 2005; Pausata et al., 2011b; Ullman et al., 2014). Therefore it is likely that inter-model differences in paleo-ice sheet topographies impacts atmospheric circulation, high-latitude simulated precipitation $\delta^{18}O$ at the Last Glacial Maximum, and thus simulated $\Delta^{18}O_{\text{ice age}}$ values reported in this study (Fig. 3).

Differences in the specification of initial seawater $\delta^{18}O$ may also lead to inter-model differences in simulated $\Delta^{18}O_{\text{ice age}}$ values. Seawater $\delta^{18}O$ is set to be globally-homogenous in CAM3Iso, IsoGSM and LMDZ, and heterogeneous in ECHAM5-wiso (using modern gridded seawater $\delta^{18}O$ heterogeneity of LeGrande and Schmidt, 2006) and GISSE2-R (coupled atmosphere–ocean model; seawater $\delta^{18}O$ is calculated by the ocean model). Simulated precipitation $\delta^{18}O$ values either show little change (±0.1 ‰) or show increases of up to 1.5 ‰ when modern spatial heterogeneous of surface ocean $\delta^{18}O$ values are included (LeGrande and Schmidt, 2006). The incorporation of heterogeneous seawater $\delta^{18}O$ into model simulations can impact simulated $\Delta^{18}O_{\text{ice age}}$ values in cases where simulated moisture sources or simulated over-ocean meteorology change between the two climate states.

The models also show deficiencies in simulating reconstructed $\Delta^{18}O_{\text{ice age}}$ values in the tropics. This finding could, in part, be related to the high sensitivity of precipitation $\delta^{18}O$ to convective parameterizations (Lee et al., 2009; Field et al., 2014), although future research is required to test this. Another reason may lie on the fact that the reconstructed $\Delta^{18}O_{\text{ice age}}$ integrates the hydroclimatological signal over multi-millennial time scales, whereas the simulated $\Delta^{18}O_{\text{ice age}}$ explicitly simulate the last glacial maximum and pre-industrial/present-day climate conditions. The stronger extra-tropical agreement between the sign of simulated and reconstructed $\Delta^{18}O_{\text{ice age}}$

CPD
11, 831–872, 2015

values (i.e., positive or negative) relative to the tropics is most likely linked to the substantial changes to extra-tropical ice-sheet topography and sea-ice cover between the two climate states in northern North America and Europe. In this case the extreme temperature anomaly between last glacial and pre-industrial climate largely overwhelms a potential bias induced by smearing reconstructed $\delta^{18}O_{\text{late-Holocene}}$ values and reconstructed $\delta^{18}O_{\text{ice age}}$ values over multiple millennia.

3.3 Regional reconstructed and simulated $\Delta^{18}O_{\text{ice age}}$ values

3.3.1 Australia and Oceania

Reconstructed $\Delta^{18}O_{\text{ice age}}$ values from Australia and Oceania fall between −1 and 1 ‰ (Figs. 1 and S3). Australian climate at the last ice age was more arid (Nanson et al., 1992), dustier (Chen et al., 1993) and cooler (Miller et al., 1997) than present day. Simulated $\Delta^{18}O_{\text{ice age}}$ values across Australia are variable amongst the five models. Reconstructed $\Delta^{18}O_{\text{ice age}}$ values across Oceania have been attributed to temporal changes in the strength of monsoons and convective rains (Aggarwal et al., 2004; Partin et al., 2007; Williams et al., 2010) potentially impacted by ice-age-to-late-Holocene shifts in the position of the intertropical convergence zone (Lewis et al., 2010, 2011).

3.3.2 Southeast Asia

Reconstructed $\Delta^{18}O_{\text{ice age}}$ values from southeast Asia range from −2.4 to +1.8 ‰. The highest regional reconstructed $\Delta^{18}O_{\text{ice age}}$ values are found in Bangladesh (reconstructed $\Delta^{18}O_{\text{ice age}}$ of +1.5 ‰ ; Aggarwal et al., 2000) and in central and southeastern China (reconstructed $\Delta^{18}O_{\text{ice age}}$ of 0.3 to +1.8 ‰ ; Wang et al., 2001; Yuan et al., 2004; Dykoski et al., 2005; Cai et al., 2010; Yang et al., 2010). General circulation models have positive simulated $\Delta^{18}O_{\text{ice age}}$ values near to the Chinese

CPD
11, 831–872, 2015

coasts, but are more variable across western and northern China (Fig. 3). Chinese speleothem records show near-zero or positive reconstructed $\Delta^{18}O_{ice\ age}$ values interpreted to reflect the reduced strength of the East Asian (Wang et al., 2001; Dykoski et al., 2005; Cosford et al., 2008) or Indian monsoons (Pausata et al., 2011a). Further research examining various time periods suggests that Chinese speleothem $\delta^{18}O$ variations reflect changes to regional moisture sources and the intensity or provenance of atmospheric transport pathways (LeGrande and Schmidt, 2009; Dayem et al., 2010; Lewis et al., 2010; Maher and Thompson, 2012; Caley et al., 2014b; Tan, 2014).

Reconstructed $\Delta^{18}O_{ice\ age}$ from North China Plain groundwaters reveals a high-magnitude, negative value (reconstructed $\Delta^{18}O_{ice\ age}$ of −2.4 ‰; Zongyu et al., 2003) compared to coastal counterparts. Combining the negative reconstructed $\Delta^{18}O_{ice\ age}$ in northern China (Zongyu et al., 2003; Ma et al., 2008; Currell et al., 2012) with the positive reconstructed $\Delta^{18}O_{ice\ age}$ values in central and southeastern China (Wang et al., 2001; Yuan et al., 2004; Dykoski et al., 2005; Cai et al., 2010; Yang et al., 2010) reveals a south-to-north decrease from positive (south) to negative (north) reconstructed $\Delta^{18}O_{ice\ age}$ values (Fig. 1). Previous studies of modern precipitation have identified increasing precipitation $\delta^{18}O$ values from the coast (i.e., Hong Kong) to inland China (e.g., Zhangye) during the wet season, sharply contrasting spatial patterns expected from Rayleigh distillation (Aragúas-Aragúas et al., 1998). More recent work suggests that low wet-season precipitation $\delta^{18}O$ values over southern China are controlled by the deflection of westerlies from the Tibetan Plateau, whereas precipitation $\delta^{18}O$ values over northern China are controlled by local-scale precipitation fluxes and raindrop evaporation (Lee et al., 2012). Therefore, reconstructed $\Delta^{18}O_{ice\ age}$ values from southern China may reflect changes to atmospheric circulation at broader spatial scales, whereas reconstructed $\Delta^{18}O_{ice\ age}$ values from northern China may indicate changes to more localized atmospheric conditions impacting processes such as raindrop evaporation in addition to meso- and synoptic-scale circulation changes.

CPD
11, 831–872, 2015

3.3.3 Africa

Reconstructed $\Delta^{18}O_{ice\ age}$ values from Africa range from −2.9 to +0.4 ‰ (Fig. 1). 14 of 18 reconstructed $\Delta^{18}O_{ice\ age}$ values from Africa are negative. Near-zero reconstructed $\Delta^{18}O_{ice\ age}$ values are generally found near to coasts (e.g., Senegal, $\Delta^{18}O_{ice\ age}$ of +0.3 ‰ ; Madioune et al., 2014), whereas higher magnitude, negative reconstructed $\Delta^{18}O_{ice\ age}$ values in Africa are found farther inland (e.g., Niger, $\Delta^{18}O_{ice\ age}$ of −3.0 ‰: ∼ 800 kilometers from the Atlantic coast). General circulation models show poorer agreement with reconstructed $\Delta^{18}O_{ice\ age}$ values over tropical Africa compared to Europe and North America (Fig. 3), mechanisms driving this extra-tropical/tropical difference remain elusive and can be examined through future inter-model or model-reconstruction comparative studies.

Northern African hydrological processes are influenced by multiple interlinked controls such as the strength of Atlantic meridional overturning circulation (Mulitza et al., 2008) and meridional shifts in the position of the intertropical convergence zone (Arbuszewski et al., 2013). Paleowater chemistry indicates that northern Africa was at least 2 °C cooler than today (Guendouz et al., 1998) and that westerly moisture transport was stronger than the present during the last ice age (Sultan et al., 1997; Abouelmagd et al., 2014). Paleowater isotope compositions of Northern Africa may have been impacted by higher-than-modern sea surface humidity as interpreted from lower-than-modern paleowater deuterium excess values (Rozanski, 1985). However, the deuterium excess of seawater during the last ice age may have been different from present day given that the Laurentide ice sheet had a deuterium excess value of ∼ 10 to ∼ 15 ‰ (e.g., Grasby and Chen, 2005; Ferguson et al., 2007).

Tropical Africa was 2–4 °C cooler and more arid than present day at the last glacial maximum (Powers et al., 2005; Tierney et al., 2008). Early- and late-Holocene precipitation fluxes and isotope compositions were highly variable across Africa (Tierney et al., 2008, 2013; Schefuß et al., 2011; Otto-Bliesner et al., 2014). Tropical African rainfall originates from both Indian and Atlantic sources, with Atlantic-sourced

CPD
11, 831–872, 2015

moisture travelling across the Congo rainforest (Levin et al., 2009). Lower-than-modern continental moisture recycling during the last ice age may partially explain negative reconstructed $\Delta^{18}O_{ice\ age}$ values across some regions of inland tropical Africa (e.g., Risi et al., 2013). Although negative reconstructed $\Delta^{18}O_{ice\ age}$ values in tropical Africa could be interpreted to reflect higher-than-modern upwind rainout during the last ice age (see Risi et al., 2008, 2010b; Lee et al., 2009; Scholl et al., 2009; Lekshmy et al., 2014; Samuels-Crow et al., 2014), this explanation necessitates stronger-than-modern convection during the last ice age, an explanation that would contradict the established cooler-than-modern land surface temperatures. Therefore, changes to atmospheric transport distances and vapor origins are more likely responsible for negative reconstructed $\Delta^{18}O_{ice\ age}$ values across tropical Africa (Lewis et al., 2010).

3.3.4 Europe and the Mediterranean

Reconstructed $\Delta^{18}O_{ice\ age}$ values across Europe, the Middle-East and the eastern Mediterranean range from −5.7 to +1.3 ‰. 80 % of reconstructed $\Delta^{18}O_{ice\ age}$ values across these regions are negative. All five general circulation models converge upon negative simulated $\Delta^{18}O_{ice\ age}$ values across Europe, consistent with the negative reconstructed $\Delta^{18}O_{ice\ age}$ values across the majority of Europe. Reconstructed $\Delta^{18}O_{ice\ age}$ values are generally higher in western Europe (0.0 to −1.0 ‰ across Portugal and the UK and France) than in eastern Europe (−1.8 to −5.7 ‰ in Poland, Hungary and Turkey), consistent with enhanced isotopic distillation of westerlies due to cooler-than-modern final condensation temperatures.

The highest magnitude, negative reconstructed $\Delta^{18}O_{ice\ age}$ value in Europe is located in Turkey near to the Black Sea (−5.7 ‰) and potentially reflects a change to regional moisture source (Fleitmann et al., 2009; Arslan et al., 2013). Westerly air mass trajectories distal to the Fennoscandian ice sheet topography have not changed considerably since the last ice age over western and central Europe (Rozanski, 1985; Loosli et al., 2001). Positive reconstructed $\Delta^{18}O_{ice\ age}$ values in the eastern

CPD
11, 831–872, 2015

Mediterranean (Frumkin et al., 1999; Bar-Matthews et al., 2003; Ayalon et al., 2013) differ from negative reconstructed $\Delta^{18}O_{ice\ age}$ values in nearby groundwater aquifers (e.g., Burg et al., 2013), advocating for further comparative research to ensure speleothem and groundwater isotope compositions each capture meteoric water $\delta^{18}O$ unaltered by fractionating processes such as partial evaporation. Recent work suggests that speleothem $\delta^{18}O$ data may be impacted by disequilibrium isotope effects (Asrat et al., 2008; Daëron et al., 2011; Kluge and Affek, 2012; Kluge et al., 2013) or by partial evaporation of drip waters resulting in ^{18}O-enrichment (e.g., Cuthbert et al., 2014a) and greater fractionation due to evaporative cooling (Cuthbert et al., 2014b), potentially explaining a portion of the difference between groundwater and speleothem reconstructed $\Delta^{18}O_{ice\ age}$ values.

Changes to freeze–thaw conditions of the ground surface between last ice age and modern climates may have impacted the seasonality of the fraction of precipitation recharging aquifers and thus $\Delta^{18}O_{ice\ age}$ (Darling, 2004, 2011; Jasechko et al., 2014). Geomorphic evidence suggests permafrost covered portions of Hungary at the last glacial maximum, suppressing land temperatures by as much as 15 °C (Fábián et al., 2014). European pollen records indicate that northern Europe was tundra-like and that southern Europe was semi-arid at the last glacial maximum (Harrison and Prentice, 2003; Clark et al., 2012). The European glacial-to-modern transition from semi-arid deserts to temperate forests could have lowered $\Delta^{18}O_{ice\ age}$ values as groundwater recharge ratios transitioned from more extreme winter-biased groundwater recharge ratios (e.g., semi-arid lands during last ice age) to less extreme but still winter-biased groundwater recharge ratios (e.g., forests during late-Holocene; Jasechko et al., 2014).

3.3.5 South America

Reconstructed $\Delta^{18}O_{ice\ age}$ values across South America range from −6.2 to 0.3‰ (Fig. 1). The highest-magnitude, negative reconstructed $\Delta^{18}O_{ice\ age}$ values (Andean ice cores; Thompson et al., 1995, 1998) are found in similar locations to the lowest present

CPD
11, 831–872, 2015

day precipitation $\delta^{18}O$ values across South America (Bowen and Wilkinson, 2002). Here the importance of upstream convection upon modern Andean precipitation $\delta^{18}O$ has been highlighted at inter-annual (e.g., Hoffmann et al., 2003; Vuille and Werner, 2005), seasonal (e.g., Vimeux et al., 2005; Samuels-Crow et al., 2014) and daily time scales (e.g., Vimeux et al., 2011). It is therefore possible that upstream convection controls past changes to Andean precipitation isotope compositions recorded in ice cores. Further, upwind changes to continental moisture recycling driven by shifts in plant transpiration fluxes may have altered continental gradients in precipitation $\delta^{18}O$. Glacial–interglacial changes to the density of Amazonian vegetation are supported by oceanic pollen records (Haberle and Maslin, 1999). Negative reconstructed $\Delta^{18}O_{\text{ice age}}$ values in parts of South America may have been driven in part by lower-than-modern continental moisture recycling during the last ice age.

The reconstructed groundwater $\Delta^{18}O_{\text{ice age}}$ value located in eastern Brazil is −2.7 ‰ (Salati et al., 1974). Eastern Brazil was 5 °C cooler than today during the last ice age (Stute et al., 1995b). Four of the five general circulation models simulate positive $\Delta^{18}O_{\text{ice age}}$ values across eastern Brazil (Fig. 3), highlighting differences between simulated and reconstructed $\Delta^{18}O_{\text{ice age}}$ values in parts of the tropics. The negative reconstructed $\Delta^{18}O_{\text{ice age}}$ value in eastern Brazil has been previously interpreted to reflect higher-than-modern precipitation during the Pleistocene (Salati et al., 1974). Lewis et al. (2010) show that localized precipitation fluxes govern precipitation $\delta^{18}O$ in east Brazil. Modern precipitation $\delta^{18}O$ values are lowest in eastern Brazil when precipitation rates are at a maximum; extending Lewis et al.'s interpretation linking local precipitation amount to precipitation $\delta^{18}O$ suggests the negative reconstructed $\Delta^{18}O_{\text{ice age}}$ value found in eastern Brazil may record wetter-than-modern conditions at the last ice age as proposed by Salati et al. (1974).

CPD
11, 831–872, 2015

3.3.6 North America

Reconstructions of $\Delta^{18}O_{ice\ age}$ from North American proxy records range from −5.5 to +1.0 ‰. Canadian records of subglacial recharge from the Laurentide ice sheet (e.g., Grasby and Chen, 2005; Ferguson et al., 2007) are not included in this synthesis because of possible transport along paleo-glacial flow paths in the Laurentide ice sheet.

Reconstructed $\Delta^{18}O_{ice\ age}$ values along the USA east coast show the highest, positive values in Georgia (latitude: 32° N; reconstructed $\Delta^{18}O_{ice\ age}$ of +1.0 ‰; Clark et al., 1997), decreasing northward to near-zero reconstructed $\Delta^{18}O_{ice\ age}$ values in coastal Maryland (latitude 39° N; reconstructed $\Delta^{18}O_{ice\ age}$ of −0.1 ‰; Aeschbach-Hertig et al., 2002). Decreasing $\Delta^{18}O_{ice\ age}$ values with increasing latitude along the USA east coast may be explained in part by the isotopic distillation of air masses advected northward from the subtropics under cooler-than-modern final atmospheric condensation temperatures. The chemistry of Maryland groundwaters has been interpreted to show that the region was more arid and 9–12 °C cooler during the last ice age relative to modern climate conditions (Purdy et al., 1996; Aeschbach-Hertig et al., 2002; Plummer et al., 2012). This glacial-to-modern temperature change is larger than most other temperature proxy records at similar latitudes (Annan and Hargreaves, 2013). Impacts of higher-than-modern ice age seawater $\delta^{18}O$ upon terrestrial precipitation $\Delta^{18}O_{ice\ age}$ may have been offset by lower sea levels that increased atmospheric transport distances during the last ice age (Clark et al., 1997; Aeschbach-Hertig et al., 2002; Tharammal et al., 2012).

Reconstructions of $\Delta^{18}O_{ice\ age}$ values in the central and southwestern USA have the highest magnitude, negative reconstructed $\Delta^{18}O_{ice\ age}$ values of temperate North America, ranging from −0.7 to −3.4 ‰. Central and southwestern USA reconstructed $\Delta^{18}O_{ice\ age}$ values contrast the positive reconstructed $\Delta^{18}O_{ice\ age}$ values found along the eastern USA coast at similar latitudes. Consistently negative $\Delta^{18}O_{ice\ age}$ values in central and southwest USA suggest that advected moisture to the region underwent

CPD
11, 831–872, 2015

greater upstream air mass distillation during the last ice age than under modern climate. Pollen, vadose zone and groundwater records show that Pleistocene southwestern USA was ~4 °C cooler, had greater groundwater recharge fluxes, and had more widespread forests than present day (Stute et al., 1992, 1995a; Scanlon et al., 2003; Williams, 2003). Negative reconstructed $\Delta^{18}O_{ice\ age}$ values found in the southwest USA have been ascribed to lower-than-modern summer precipitation (New Mexico, Phillips et al., 1986), latitudinal shifts in the positions of the polar jet stream and the intertropical convergence zone (New Mexico, Asmerom et al., 2010) and changes to over-ocean humidity, temperature or moisture sources (Idaho, Schlegel et al., 2009). USA reconstructed $\Delta^{18}O_{ice\ age}$ values could also be influenced by changes to groundwater recharge ratio seasonality as land surface conditions changed (Jasechko et al., 2014). Wagner et al. (2010) interpret decreases to southwestern precipitation $\delta^{18}O$ to reflect cooler and more-humid conditions. Extending this interpretation to negative reconstructed $\Delta^{18}O_{ice\ age}$ across the southwestern USA values supports earlier conclusions that the region was cooler and more humid than today during the last ice age, possibly linked to changes in air mass trajectories and moisture sources (Asmerom et al., 2010; Wagner et al., 2010).

Simulated $\Delta^{18}O_{ice\ age}$ values across North America closely match spatial patterns of reconstructed $\Delta^{18}O_{ice\ age}$ synthesized in this study. The strong, multi-model agreement with reconstructed $\Delta^{18}O_{ice\ age}$ values support continued application of isotope enabled general circulation models when interpreting USA precipitation isotope proxy records.

4 Conclusions

Compiled groundwater, speleothem, ice core and ground ice records of $\delta^{18}O$ changes between the last ice age and the late-Holocene range from −7.1 (i.e., $\delta^{18}O_{ice\ age} < \delta^{18}O_{late\text{-}Holocene}$) to +1.8 ‰ (i.e., $\delta^{18}O_{ice\ age} > \delta^{18}O_{late\text{-}Holocene}$). Aquifers with positive reconstructed $\Delta^{18}O_{ice\ age}$ values (25 % of records) are most common along the

CPD
11, 831–872, 2015

subtropical coasts. 75 % of reconstructed $\Delta^{18}O_{ice\ age}$ values are negative, with the highest magnitude differences between $\delta^{18}O_{ice\ age}$ and $\delta^{18}O_{late\text{-}Holocene}$ observed at high latitudes and far from coasts. This spatial pattern suggests stronger isotopic distillation of advected air masses during the last ice age than under present climate were able to override higher-than-modern glacial seawater $\delta^{18}O$ values at most locations. Future paleo-precipitation proxy record $\delta^{18}O$ research can use this new global map of $\Delta^{18}O_{ice\ age}$ records to target and prioritize developing new records in certain regions and to compare $\Delta^{18}O_{ice\ age}$ shifts from different proxy records. In the near term, a global compilation of large lake sediment isotope records that accounts for paleo-evaporative isotope effects could enhance spatial coverage of interglacial-glacial $\delta^{18}O$ shifts.

General circulation models agree on the sign and magnitude of terrestrial precipitation $\Delta^{18}O_{ice\ age}$ values better in the extra-tropics than in the tropics. Differences in simulated precipitation isotope composition changes amongst the models might be linked to different parameterizations of seawater $\delta^{18}O$, glacial topography and convective rainfall, however, this hypothesis requires further testing. Future model research should focus on quantifying the relative roles of inter-model spread in the simulated climate vs. the isotopic response to climate change on resulting simulated precipitation $\delta^{18}O$. This would provide guidelines to interpret model-data isotopic differences and to identify what aspects of the ice age climate and hydrology models have difficulties in capturing.

The Supplement related to this article is available online at doi:10.5194/cpd-11-831-2015-supplement.

Acknowledgements. UNESCO IGCP-618 project (Paleoclimate information obtained from past-recharged groundwater), the G@GPS network and the Caswell Silver Foundation are acknowledged for their financial support.

CPD
11, 831–872, 2015

References

Abouelmagd, A., Sultan, M. Milewski, A., Kehew, A. E., Sturchio, N. C., Soliman, F., Krishnamurthy, R. V., and Cutrim, E.: Toward a better understanding of palaeoclimatic regimes that recharged the fossil aquifers in North Africa: inferences from stable isotope and remote sensing data, Palaeogeogr. Palaeocl., 329–330, 137–149, 2012.

Aeschbach-Hertig, W., Stute, M., Clark, J. F., Reuter, R. F., and Schlosser, P.: A paleotemperature record derived from dissolved noble gases in groundwater of the Aquia Aquifer (Maryland, USA), Geochim. Cosmochim. Ac., 66, 797–817, 2002.

Aggarwal, P. K., Basu, A. R., Poreda, R. J., Kulkarni, K. M., Froehlich, K., Tarafdar, S. A., Ali, M., Ahmed, N., Hussain, A., Rahman, M., and Ahmed, S. R.: A report on isotope hydrology of groundwater in Bangladesh: implications for characterization and mitigation of arsenic in groundwater, International Atomic Energy Agency, Department of Technical Co-operation, Vienna (Austria), 2000.

Aggarwal, P. K., Fröhlich, K., Kulkarni, K. M., and Gourcy, L. L.: Stable isotope evidence for moisture sources in the Asian summer monsoon under present and past climate regimes, Geophys. Res. Lett., 31, L08203, doi:10.1029/2004GL019911, 2004.

Akouvi, A., Dray, M., Violette, S., de Marsily, G., and Zuppi, G. M.: The sedimentary coastal basin of Togo: example of a multilayered aquifer still influenced by a palaeo-seawater intrusion, Hydrogeol. J., 16, 419–436, 2008.

Anderson, L., Abbott, M. B., and Finney, B. P.: Holocene climate inferred from oxygen isotope ratios in lake sediments, central Brooks Range, Alaska, Quaternary Res., 55, 313–321, 2001.

Annan, J. D. and Hargreaves, J. C.: A new global reconstruction of temperature changes at the Last Glacial Maximum, Clim. Past, 9, 367–376, doi:10.5194/cp-9-367-2013, 2013.

Aragúas-Aragúas, L., Froehlich, K., and Rozanski, K.: Stable isotope composition of precipitation over Southeast Asia, J. Geophys. Res., 103, 721–742, 1998.

Arbuszewski, J. A., Cléroux, C., Bradtmiller, L., and Mix, A.: Meridional shifts of the Atlantic intertropical convergence zone since the Last Glacial Maximum, Nat. Geosci., 6, 959–962, 2013.

Argus, D. F. and Peltier, W. R.: Constraining models of postglacial rebound using space geodesy: a detailed assessment of model ICE-5G (VM2) and its relatives, Geophys. J. Int., 181, 697–723, 2010.

CPD
11, 831–872, 2015

Arslan, S., Yazicigil, H., Stute, M., and Schlosser, P.: Environmental isotopes and noble gases in the deep aquifer system of Kazan Trona Ore Field, Ankara, central Turkey and links to paleoclimate, Quaternary Res., 79, 292–303, 2013.

Asmerom, Y., Polyak, V. J., and Burns, S. J.: Variable winter moisture in the southwestern United States linked to rapid glacial climate shifts, Nat. Geosci., 3, 114–117, 2010.

Asrat, A., Baker, A., Leng, M., Gunn, J., and Umer, M.: Environmental monitoring in the Mechara caves, Southeastern Ethiopia: implications for speleothem palaeoclimate studies, Int. J. Speleol., 37, 207–220, 2008.

Ayalon, A., Bar-Matthews, M., Frumkin, A., and Matthews, A.: Last Glacial warm events on Mount Hermon: the southern extension of the Alpine karst range of the east Mediterranean, Quaternary Sci. Rev., 59, 43–56, 2013.

Bakari, S. S., Aagaard, P., Vogt, R. D., Ruden, F., Brennwald, M. S., Johansen, I., and Gulliksen, S.: Groundwater residence time and paleorecharge conditions in the deep confined aquifers of the coastal watershed, South-East Tanzania, J. Hydrol., 466–467, 127–140, 2012.

Bar-Matthews, M., Ayalon, A., Gilmour, M., Matthews, A., and Hawkesworth, C.: Sea–land oxygen isotopic relationships from planktonic foraminifera and speleothems in the Eastern Mediterranean region and their implication for paleorainfall during interglacial intervals, Geochim. Cosmochim. Ac., 67, 3181–3199, 2003.

Beuning, K. R., Kelts, K., Russell, J. M., and Wolfe, B. B.: Reassessment of Lake Victoria–Upper Nile River paleohydrology from oxygen isotope records of lake-sediment cellulose, Geology, 30, 559–562, 2002.

Bowen, G. J. and Wilkinson, B.: Spatial distribution of δ^{18}O in meteoric precipitation, Geology, 30, 315–318, 2002.

Braconnot, P., Otto-Bliesner, B., Harrison, S., Joussaume, S., Peterchmitt, J.-Y., Abe-Ouchi, A., Crucifix, M., Driesschaert, E., Fichefet, T., Hewitt, C. D., Kageyama, M., Kitoh, A., Laîné, A., Loutre, M.-F., Marti, O., Merkel, U., Ramstein, G., Valdes, P., Weber, S. L., Yu, Y., and Zhao, Y.: Results of PMIP2 coupled simulations of the Mid-Holocene and Last Glacial Maximum – Part 1: experiments and large-scale features, Clim. Past, 3, 261–277, doi:10.5194/cp-3-261-2007, 2007.

Braconnot, P., Harrison, S. P., Kageyama, M., Bartlein, P. J., Masson-Delmotte, V., Abe-Ouchi, A. Otto-Bliesner, B., and Zhao, Y.: Evaluation of climate models using palaeoclimatic data, Nature Climate Change, 2, 417–424, 2012. (NOT FOUND!)

CPD
11, 831–872, 2015

Burg, A., Zilderbrand, M., Yechieli, Y.: Radiocarbon variability in groundwater in an extremely arid zone – the Arava Valley, Israel, Radiocarbon, 55, 963–978, 2013.
Cai, Y., Tan, L., Cheng, H., An, Z., Edwards, R. L., Kelly, M. J., Kong, X., and Wang, X.: The variation of summer monsoon precipitation in central China since the last deglaciation, Earth Planet. Sc. Lett., 291, 21–31, 2010.
Caley, T., Roche, D. M., Waelbroeck, C., and Michel, E.: Oxygen stable isotopes during the Last Glacial Maximum climate: perspectives from data–model (*i*LOVECLIM) comparison, Clim. Past, 10, 1939–1955, doi:10.5194/cp-10-1939-2014, 2014a.
Caley, T., Roche, D. M., Renssen, H.: Orbital Asian summer monsoon dynamics revealed using an isotope-enabled global climate model, Nat. Commun., 10, 105–148, 2014b. (NOT FOUND!)
Chen, X. Y., Bowler, J. M., and Magee, J. W.: Late Cenozoic stratigraphy and hydrologic history of Lake Amadeus, a central Australian playa, Aust. J. Earth Sci., 40, 1–14, 1993.
Ciais, P. and Jouzel, J.: Deuterium and oxygen 18 in precipitation: isotopic model, including mixed cloud processes, J. Geophys. Res., 99, 16793–16803, 1994.
Clark, J. F., Stute, M., Schlosser, P., Drenkard, S., and Bonani, G.: A tracer study of the Floridan aquifer in southeastern Georgia: implications for groundwater flow and paleoclimate, Water Resour. Res., 33, 281–289, 1997.
Clark, P. U., Dyke, A. S., Shakun, J. D., Carlson, A. E., Clark, J., Wohlfarth, B., Mitrovica, J. X., Hostetler, W. S., and McCabe, A. M.: The last glacial maximum, Science, 325, 710–714, 2009.
Clark, P. U., Shakun, J. D., Baker, P. A., Bartlein, P. J., Brewer, S., Brook, E., Carlson, A. E., Cheng, H., Kaufman, D. S., Liu, Z., Marchitto, T. M., Mix, A. C., Morrill, C., Otto-Bliesner, B. L., Pahnke, K., Russell, J. M., Whitlock, C., Adkins, J. F., Blois, J. L., Clark, J., Colman, S. M., Curry, W. B., Flower, B. P., He, F., Johnson, T. C., Lynch-Stieglitz, J., Markgraf, V., McManus, J., Mitrovica, J. X., Moreno, P. I., and Williams, J. W.: Global climate evolution during the last deglaciation, P. Natl. Acad. Sci. USA, 109, E1134–E1142, 2012.
Corcho Alvarado, J. A., Leuenberger, M., Kipfer, R., Paces, T., and Purtschert, R.: Reconstruction of past climate conditions over central Europe from groundwater data, Quaternary Sci. Rev., 30, 3423–3429, 2011.
Cosford, J., Qing, H., Yuan, D., Zhang, M., Holmden, C., Patterson, W., and Hai, C.: Millennial-scale variability in the Asian monsoon: evidence from oxygen isotope records from stalagmites in southeastern China, Palaeogeogr. Palaeocl., 266, 3–12, 2008.

CPD
11, 831–872, 2015

Cruz, F. W., Burns, S. J., Karmann, I., Sharp, W. D., Vuille, M., Cardoso, A. O., Ferrari, J. A., Dias, P. L. S., and Viana, O.: Insolation-driven changes in atmospheric circulation over the past 116,000 years in subtropical Brazil, Nature, 434, 63–66, 2005.

Currell, M. J., Han, D., Chen, Z., and Cartwright, I.: Sustainability of groundwater usage in northern China: dependence on palaeowaters and effects on water quality, quantity and ecosystem health, Hydrol. Process., 26, 4050–4066, 2012.

Currell, M., Cendón, D. I., and Cheng, X.: Analysis of environmental isotopes in groundwater to understand the response of a vulnerable coastal aquifer to pumping: Western Port Basin, south-eastern Australia, Hydrogeol. J., 21, 1413–1427, 2013.

Cuthbert, M. O., Baker, A., Jex, C. N., Graham, P. W., Treble, P. C., Andersen, M. S., and Acworth, I. R.: Drip water isotopes in semi-arid karst: implications for speleothem paleoclimatology, Earth Planet. Sc. Lett., 395, 194–204, 2014a.

Cuthbert, M. O., Rau, G. C., Andersen, M. S., Roshan, H., Rutlidge, H., Marjo, C. E., Markowska, M., Jex, C. N., Graham, P. W., Mariethoz, G., Acwoth, R. I., and Baker, A.: Evaporative cooling of speleothem drip water, Sci. Rep., 4, 5162, 2014b. (NOT FOUND!)

Daëron, M., Guo, W., Eiler, J., Genty, D., Blamart, D., Boch, R., Drysdale, R., Maire, R., Wainer, K., and Zanchetta, G.: $^{13}C^{18}O$ clumping in speleothems: observations from natural caves and precipitation experiments, Geochim. Cosmochim. Ac., 75, 3303–3317, 2011.

Dansgaard, W.: Stable isotopes in precipitation, Tellus, 16, 436–468, 1964.

Dansgaard, W. and Tauber, H.: Glacier oxygen-18 content and Pleistocene ocean temperatures, Science, 166, 499–502, 1969.

Dansgaard, W., Clausen, H. B., Gundestrup, N., Hammer, C. U., Johnsen, S. F., Kristinsdottir, P. M., and Reeh, N.: A new Greenland deep ice core, Science, 218, 1273–1277, 1982.

Darling, W. G.: Hydrological factors in the interpretation of stable isotopic proxy data present and past: a European perspective, Quaternary Sci. Rev., 23, 743–770, 2004.

Darling, W. G.: The isotope hydrology of quaternary climate change, J. Hum. Evol., 60, 417–427, 2011.

Davison, M. R. and Airey, P. L.: The effect of dispersion on the establishment of a paleoclimatic record from groundwater, J. Hydrol., 58, 131–147, 1982.

Dayem, K. E., Molnar, P., Battisti, D. S., and Roe, G. H.: Lessons learned from oxygen isotopes in modern precipitation applied to interpretation of speleothem records of paleoclimate from eastern Asia, Earth Planet. Sc. Lett., 295, 219–230, 2010.

CPD
11, 831–872, 2015

Denniston, R. F., González, L. A., Asmerom, Y., Sharma, R. H., and Reagan, M. K.: Speleothem evidence for changes in Indian summer monsoon precipitation over the last ~2300 years, Quaternary Res., 53, 196–202, 2000.
Dykoski, C. A., Edwards, R. L., Cheng, H., Yuan, D., Cai, Y., Zhang, M., Lin, Y., Qing, J., An, Z., and Revenaugh, J.: A high-resolution, absolute-dated Holocene and deglacial Asian monsoon record from Dongge Cave, China, Earth Planet. Sc. Lett., 233, 71–86, 2005.
Eawag, A. F., Eicher, U., Siegenthaler, U., and Birks, H. J. B.: Late-glacial climatic oscillations as recorded in Swiss lake sediments, J. Quaternary Sci., 7, 187–204, 1992.
Edmunds, W. M.: Palaeoclimate and groundwater evolution in Africa – implications for adaptation and management, Hydrolog. Sci. J., 54, 781–792, 2009.
Edmunds, W. M. and Milne, C. (Eds.): Palaeowaters in coastal Europe: evolution of Groundwater since the late Pleistocene, Geol. Society Special. Publication, 189, Geological Society of London, London, 2001.
Edwards, T. W. D. and McAndrews, J. H.: Paleohydrology of a Canadian Shield lake inferred from ^{18}O in sediment cellulose, Can. J. Earth Sci., 26, 1850–1859, 1989.
Emiliani, C.: Pleistocene temperatures, J. Geol., 63, 538–578, 1955.
Fábián, S. Á., Kovács, J., Varga, G., Sipos, G., Horváth, Z., Thamó-Bozsó, E., and Tóth, G.: Distribution of relict permafrost features in the Pannonian Basin, Hungary, Boreas, 43, 722–732, 2014.
Fawcett, P. J., Ágústsdóttir, A. M., Alley, R. B., and Shuman, C. A.: The Younger Dryas termination and North Atlantic Deep Water formation: insights from climate model simulations and Greenland ice cores, Paleoceanography, 12, 23–38, 1997.
Feng, W., Casteel, R. C., Banner, J. L., and Heinze-Fry, A.: Oxygen isotope variations in rainfall, drip-water and speleothem calcite from a well-ventilated cave in Texas, USA: assessing a new speleothem temperature proxy, Geochim. Cosmochim. Ac., 127, 233–250, 2014.
Ferguson, G. A., Betcher, R. N., and Grasby, S. E.: Hydrogeology of the Winnipeg formation in Manitoba, Canada, Hydrogeol. J., 15, 573–587, 2007.
Field, R. D., Kim, D., LeGrande, A. N., Worden, J., Kelley, M., and Schmidt, G. A.: Evaluating climate model performance in the tropics with retrievals of water isotopic composition from Aura TES, Geophys. Res. Lett., 41, 6030–6036, 2014.
Fleitmann, D., Cheng, H., Badertscher, S., Edwards, R. L., Mudelsee, M., Göktürk, O. M., Fankhauser, A., Pickering, R., Raible, C. C., Matter, A., Kramers, J., and Tüysüz, O.: Timing

CPD
11, 831–872, 2015

and climatic impact of Greenland interstadials recorded in stalagmites from northern Turkey, Geophys. Res. Lett., 36, L19707, doi:10.1029/2009GL040050, 2009.
Frumkin, A., Ford, D. C., and Schwarcz, H. P.: Continental oxygen isotopic record of the last 170,000 years in Jerusalem, Quaternary Res., 51, 317–327, 1999.
Garreaud, R. D., Vuille, M., Compagnucci, R., and Marengo, J.: Present-day south american climate, Palaeogeogr. Palaeocl., 281, 180–195, 2009.
Gat, J. R., Mazor, E., and Tzur, Y.: The stable isotope composition of mineral waters in the Jordan Rift Valley, J. Hydrol., 7, 334–352, 1969.
Gibson, J. J., Birks, S. J., and Edwards, T. W. D.: Global prediction of δ_A and δ^2H-δ^{18}O evaporation slopes for lakes and soil water accounting for seasonality, Global Biogeochem. Cy., 22, GB2031, doi:10.1029/2007GB002997, 2008.
Grasby, S. E. and Chen, Z.: Subglacial recharge into the Western Canada Sedimentary Basin – impact of Pleistocene glaciation on basin hydrodynamics, Geol. Soc. Am. Bull., 117, 500–514, 2005.
Guendouz, A., Moulla, A. S., Edmunds, W. M., Shand, P., Poole, J., Zouari, K., and Mamou, A.: Palaeoclimatic information contained in groundwaters of the Grnad Erg Oriental, northern Africa, in: Isotope Techniques in the study of Environmental Change, International Atomic Energy Agency, Vienna, 1998.
Haberle, S. G. and Maslin, M. A.: Late Quaternary vegetation and climate change in the Amazon basin based on a 50,000 year pollen record from the Amazon fan, ODP site 932, Quaternary Res., 51, 27–38, 1999.
Hamouda, M. F. B., Tarhouni, J., Leduc, C., and Zouari, K.: Understanding the origin of salinization of the Plio-quaternary eastern coastal aquifer of Cap Bon (Tunisia) using geochemical and isotope investigations, Environ. Earth Sci., 63, 889–901, 2011. (NOT FOUND!)
Han, D., Kohfahl, C., Song, X., Xiao, G., and Yang, J.: Geochemical and isotopic evidence for palaeo-seawater intrusion into the south coast aquifer of Laizhou Bay, China, Appl. Geochem., 26, 863–883, 2011.
Harmon, R. S., Thompson, P., Schwarcz, H. P., and Ford, D. C.: Late Pleistocene paleoclimates of North America as inferred from stable isotope studies of speleothems, Quaternary Res., 9, 54–70, 1978.
Harmon, R. S., Schwarcz, H. P., Ford, D. C., and Koch, D. L.: An isotopic paleotemperature record for late Wisconsinan time in northeast Iowa, Geology, 7, 430–433, 1979.

CPD
11, 831–872, 2015

Harrison, S. P. and Prentice, I. C.: Climate and CO_2 controls on global vegetation distribution at the last glacial maximum: analysis based on palaeovegetation data, biome modelling and palaeoclimate simulations, Glob. Change Biol., 9, 983–1004, 2003.

Hoffmann, G., Ramirez, E., Taupin, J. D., Francou, B., Ribstein, P., Delmas, R., Dürr, H., Gallaire, R., Simões, J., Schotterer, U., Stievenard, M., and Werner, M.: Coherent isotope history of Andean ice cores over the last century, Geophys. Res. Lett., 30, 1179, doi:10.1029/2002GL014870, 2003.

Jasechko, S., Birks, S. J., Gleeson, T., Wada, Y., Fawcett, P. J., Sharp, Z. D., McDonnell, J. J., and Welker, J. M.: The pronounced seasonality of global groundwater recharge, Water Resour. Res., 50, 8845–8867, 2014.

Jiráková, H., Huneau, F., Celle-Jeanton, H., Hrkal, Z., and La Coustumer, P. L.: Insights into palaeorecharge conditions for European deep aquifers, Hydrogeol. J., 19, 1545–1562, 2011.

Johnsen, S. J., Dahl-Jensen, D., Gundestrup, N., Steffensen, J. P., Clausen, H. B., Miller, H., Masson-Delmotte, V., Sveinbjörnsdottir, A. E., and White, J.: Oxygen isotope and palaeotemperature records from six Greenland ice-core stations: Camp Century, Dye-3, GRIP, GISP2, Renland and NorthGRIP, J. Quaternary Sci., 16, 299–307, 2001.

Jouzel, J., Hoffmann, G., Koster, R. D., and Masson, V.: Water isotopes in precipitation: data/model comparison for present-day and past climates, Quaternary Sci. Rev., 19, 363–379, 2000.

Justino, F., Timmermann, A., Merkel, U., and Souza, E. P.: Synoptic reorganization of atmospheric flow during the Last Glacial Maximum, J. Climate, 18, 2826–2846, 2005.

Kluge, T. and Affek, H. P.: Quantifying kinetic fractionation in Bunker Cave speleothems using Δ_{47}, Quaternary Sci. Rev., 49, 82–94, 2012.

Kluge, T., Affek, H. P., Marx, T., Aeschbach-Hertig, W., Riechelmann, D. F. C., Scholz, D., Riechelmann, S., Immenhauser, A., Richter, D. K., Fohlmeister, J., Wackerbarth, A., Mangini, A., and Spötl, C.: Reconstruction of drip-water $\delta^{18}O$ based on calcite oxygen and clumped isotopes of speleothems from Bunker Cave (Germany), Clim. Past, 9, 377–391, doi:10.5194/cp-9-377-2013, 2013.

Lachniet, M. S., Asmerom, Y., Burns, S. J., Patterson, W. P., Polyak, V. J., and Seltzer, G. O.: Tropical response to the 8200 yr BP cold event? Speleothem isotopes indicate a weakened early Holocene monsoon in Costa Rica, Geology, 32, 957–960, 2004.

CPD
11, 831–872, 2015

Lee, J.-E., Pierrehumbert, R., Swann, A., and Lintner, B. R.: Sensitivity of stable water isotopic values to convective parameterization schemes, Geophys. Res. Lett., 36, L23801, doi:10.1029/2009GL040880, 2009.

Lee, J.-E., Risi, C., Fung, I., Worden, J., Scheepmaker, R. A., Lintner, B., and Frankenberg, C.: Asian monsoon hydrometeorology from TES and SCIAMACHY water vapor isotope measurements and LMDZ simulations: implications for speleothem climate record interpretation, J. Geophys. Res., 117, D15112, doi:10.1029/2011JD017133, 2012.

LeGrande, A. N. and Schmidt, G. A.: Global gridded data set of the oxygen isotopic composition in seawater, Geophys. Res. Lett., 33, L12604, doi:10.1029/2006GL026011, 2006.

LeGrande, A. N. and Schmidt, G. A.: Ensemble, water isotope–enabled, coupled general circulation modeling insights into the 8.2 ka event, Paleoceanography, 23, PA3207, doi:10.1029/2008PA001610, 2008.

LeGrande, A. N. and Schmidt, G. A.: Sources of Holocene variability of oxygen isotopes in paleoclimate archives, Clim. Past, 5, 441–455, doi:10.5194/cp-5-441-2009, 2009.

Lekshmy, P. R., Midhun, M., Ramesh, R., and Jani, R. A: ^{18}O depletion in monsoon rain relates to large scale organized convection rather than the amount of rainfall, Scientific Reports, 4, 5661, doi:10.1038/srep05661, 2014.

Leng, M. J. and Marshall, J. D.: Palaeoclimate interpretation of stable isotope data from lake sediment archives, Quaternary Sci. Rev., 23, 811–831, 2004.

Levin, N. E., Zipser, E. J., and Cerling, T. E.: Isotopic composition of waters from Ethiopia and Kenya: insights into moisture sources for eastern Africa, J. Geophys. Res., 114, D23306, doi:10.1029/2009JD012166, 2009.

Lewis, S. C., LeGrande, A. N., Kelley, M., and Schmidt, G. A.: Water vapour source impacts on oxygen isotope variability in tropical precipitation during Heinrich events, Clim. Past, 6, 325–343, doi:10.5194/cp-6-325-2010, 2010.

Lewis, S. C., Gagan, M. K., Ayliffe, L. K., Zhao, J.-X., Hantoro, W. S., Treble, P. C., Hellstrom, J. C., LeGrande, A. N., Kelley, M., Schmidt, G. A., and Suwargadi, B. W.: High-resolution stalagmite reconstructions of Australian–Indonesian monsoon rainfall variability during Heinrich stadial 3 and Greenland interstadial 4, Earth Planet. Sc. Lett., 303, 133–142, 2011.

Licciardi, J. M., Teller, J. T., and Clark, P. U.: Freshwater routing by the Laurentide Ice Sheet during the last deglaciation, in: Mechanisms of Global Climate Change at Millennial Time

CPD
11, 831–872, 2015

Scales, edited by: Clark, P. U., Webb, R. S., and Keigwin, L. D., American Geophysical Union (AGU), Washington, D.C., AGU Geophysical Monograph 112, 177–201, 1999.

Liu, X., Shen, J., Wang, S., Wang, Y., and Liu, W.: Southwest monsoon changes indicated by oxygen isotope of ostracode shells from sediments in Qinghai Lake since the late Glacial, Chinese Sci. Bull., 52, 539–544, 2007.

Liu, Z., Yoshimura, K., Bowen, G. J., and Welker, J. M.: Pacific–North American teleconnection controls on precipitation isotopes (δ^{18}O) across the Contiguous United States and adjacent regions: a GCM-based analysis, J. Climate, 27, 1046–1061, 2014a.

Liu, Z., Yoshimura, K., Bowen, G. J., Buenning, N. H., Risi, C., Welker, J. M., and Yuan, F.: Paired oxygen isotope records reveal modern North American atmospheric dynamics during the Holocene, Nature Commun., 5, 1–7, 2014b.

Loosli, H. H., Aeschbach-Hertig, W., Barbecot, F., Blaser, P., Darling, W. G., Dever, L., Edmunds, W. M., Kipfer, R., Purtschert, R., and Walraevens, K.: Isotopic methods and their hydrogeochemical context in the investigation of palaeowaters, Geo. Soc. S. P., 189, 193–212, 2001.

Ma, J. Z., Ding, Z., Gates, J. B., and Su, Y.: Chloride and the environmental isotopes as the indicators of the groundwater recharge in the Gobi Desert, northwest China, Environ. Geol., 55, 1407–1419, 2008.

Madioune, D. H., Faye, S., Orban, P., Brouyère, S., Dassargues, A., Mudry, J., Stumpp, C., and Maloszewski, P.: Application of isotopic tracers as a tool for understanding hydrodynamic behavior of the highly exploited Diass aquifer system (Senegal), J. Hydrol., 511, 443–459, 2014.

Maher, B. A. and Thompson, R.: Oxygen isotopes from Chinese caves: records not of monsoon rainfall but of circulation regime, J. Quaternary Sci., 27, 615–624, 2012.

MARGO Members, Constraints on the magnitude and patterns of ocean cooling at the Last Glacial Maximum, Nat. Geosci., 2, 127–132, 2009.

Masson-Delmotte, V., Landais, A. Stievenard, M., Cattani, O., Falourd, S., Jouzel, J., Johnsen, S. J., Dahl-Jensen, D., Sveinsbjornsdottir, A., White, J. W. C., Popp, T., and Fischer, H.: Holocene climatic changes in Greenland: different deuterium excess signals at Greenland Ice Core Project (GRIP) and NorthGRIP, J. Geophys. Res., 110, D14102, doi:10.1029/2004JD005575, 2005.

CPD
11, 831–872, 2015

McDermott, F., Mattey, D. P., and Hawkesworth, C.: Centennial-scale Holocene climate variability revealed by a high-resolution speleothem $\delta^{18}O$ record from SW Ireland, Science, 294, 1328–1331, 2001.

Menking, K. M., Bischoff, J. L., Fitzpatrick, J. A., Burdette, J. W., and Rye, R. O.: Climatic/hydrologic oscillations since 155,000 yr BP at Owens Lake, California, reflected in abundance and stable isotope composition of sediment carbonate, Quaternary Res., 48, 58–68, 1997.

Miller, G. H., Magee, J. W., and Jull, A. J. T.: Low-latitude glacial cooling in the Southern Hemisphere from amino-acid racemization in emu eggshells, Nature, 385, 241–244, 1997.

Morley, D. W., Leng, M. J., Mackay, A. W., and Sloane, H. J.: Late glacial and Holocene environmental change in the Lake Baikal region documented by oxygen isotopes from diatom silica, Global Planet. Change, 46, 221–233, 2005.

Morrissey, S. K., Clark, J. F., Bennett, M., Richardson, E., and Stute, M.: Groundwater reorganization in the Floridan aquifer following Holocene sea-level rise, Nat. Geosci., 3, 683–687, 2010.

Mulitza, S., Prange, M., Stuut, J.-B., Zabel, M., von Dobeneck, T., Itambi, A. C., Nizou, J., Schulz, M., and Wefer, G.: Sahel megadroughts triggered by glacial slowdowns of Atlantic meridional overturning, Paleoceanography, 23, PA4206, doi:10.1029/2008PA001637, 2008.

Münnich, K. O.: Messungen des C^{14}-Gehaltes von hartem Grundwasser, Naturwissenschaften, 44, 32–33, 1957.

Münnich, K. O., Roether, W., and Thilo, L.: Dating of groundwater with tritium and ^{14}C, Isotopes in Hydrology, Proceedings of the Symposium on isotopes in hydrology, 14–18 November 1966, International Atomic Energy Agency, Vienna, 305–320, 1967.

Nanson, G., Price, D., and Short, S.: Wetting and drying of Australia over the past 300 ka, Geology, 20, 791–794, 1992.

Négrel, P. and Petelet-Giraud, E.: Isotopes in groundwater as indicators of climate changes, TRAC-Trend. Anal. Chem., 30, 1279–1290, 2011.

Nikolayev, V. I. and Mikhalev, D. V.: An oxygen-isotope paleothermometer from ice in Siberian permafrost, Quaternary Res., 43, 14–21, 1995.

Noone, D. and Sturm, C.: Comprehensive dynamical models of global and regional water isotope distributions. in: Isoscapes: understanding Movement, Pattern, and Process on Earth through Isotope Mapping, Springer, New York, 195–219, 2010.

CPD
11, 831–872, 2015

Otto-Bliesner, B. L., Russell, J. M., Clark, P. U., Liu, Z., Overpeck, J. T., Konecky, B., deMenocal, P., Nicholson, S. E., He, F., Lu, Z.: Coherent changes of southeastern equatorial and northern African rainfall during the last deglaciation, Science, 346, 1223–1227, 2014.

Partin, J. W., Cobb, K. M., Adkins, J. F., Clark, B., and Fernandez, D. P.: Millennial-scale trends in west Pacific warm pool hydrology since the Last Glacial Maximum, Nature, 449, 452–455, 2007.

Pausata, F. S. R., Li, C., Wettstein, J. J., Nisancioglu, K. H., and Battisti, D. S.: Changes in atmospheric variability in a glacial climate and the impacts on proxy data: a model intercomparison, Clim. Past, 5, 489–502, doi:10.5194/cp-5-489-2009, 2009.

Pausata, F. S. R., Battisti, D. S., Nisancioglu, K. H., and Bitz, C. M.: Chinese stalagmite δ^{18}O controlled by changes in the Indian monsoon during a simulated Heinrich event, Nat. Geosci., 4, 474–480, 2011a.

Pausata, F. S. R., Li, C., Wettstein, J. J., Kageyama, M., and Nisancioglu, K. H.: The key role of topography in altering North Atlantic atmospheric circulation during the last glacial period, Clim. Past, 7, 1089–1101, doi:10.5194/cp-7-1089-2011, 2011b.

Pearson, F. J. and White, D. E.: Carbon 14 ages and flow rates of water in Carrizo Sand, Atascosa County, Texas, Water Resour. Res., 3, 251–261, 1967.

Pedro, J. B., van Ommen, T. D., Rasmussen, S. O., Morgan, V. I., Chappellaz, J., Moy, A. D., Masson-Delmotte, V., and Delmotte, M.: The last deglaciation: timing the bipolar seesaw, Clim. Past, 7, 671–683, doi:10.5194/cp-7-671-2011, 2011.

Peltier, W. R.: Ice age paleotopography, Science, 265, 195–201, 1994.

Phillips, F. M., Peeters, L. A., Tansey, M. K., and Davis, S. N.: Paleoclimatic inferences from an isotopic investigation of groundwater in the central San Juan Basin, New Mexico, Quaternary Res., 26, 179–193, 1986.

Plummer, L. N.: Stable isotope enrichment in paleowaters of the southeast Atlantic Coastal Plain, United States, Science, 262, 2016–2020, 1993.

Plummer, L. N., Eggleston, J. R., Andreasen, D. C., Raffensperger, J. P., Hunt, A. G., and Casile, G. C.: Old groundwater in parts of the upper Patapsco aquifer, Atlantic Coastal Plain, Maryland, USA: evidence from radiocarbon, chlorine-36 and helium-4, Hydrogeol. J., 20, 1269–1294, 2012.

Powers, L. A., Johnson, T. C., Werne, J. P., Castañeda, I. S., Hopmans, E. C., Sinninghe Damsté, J. S., and Schouten, S.: Large temperature variability in the southern

CPD
11, 831–872, 2015

African tropics since the Last Glacial Maximum, Geophys. Res. Lett., 32, L08706, doi:10.1029/2004GL022014, 2005.
Purdy, C. B., Helz, G. R., Mignerey, A. C., Kubik, P. W., Elmore, D., Sharma, P., and Hemmick, T.: Aquia aquifer dissolved Cl^- and $^{36}Cl/Cl$: implications for flow velocities, Water Resour. Res., 32, 1163–1171, 1996.
Risi, C., Bony, S., Vimeux, F., Descroix, L., Ibrahim, B., Lebreton, E., Mamadou, I., and Sultan, B.: What controls the isotopic composition of the African monsoon precipitation? Insights from event-based precipitation collected during the 2006 AMMA field campaign, Geophys. Res. Lett., 35, L24808, doi:10.1029/2008GL035920, 2008.
Risi, C., Bony, S., Vimeux, F., and Jouzel, J.: Water-stable isotopes in the LMDZ4 general circulation model: model evaluation for present-day and past climates and applications to climatic interpretations of tropical isotopic records, J. Geophys. Res., 115, D12118, doi:10.1029/2009JD013255, 2010a.
Risi, C., Bony, S., Vimeux, F., Frankenberg, C., Noone, D., and Worden, J.: Understanding the Sahelian water budget through the isotopic composition of water vapor and precipitation, J. Geophys. Res., 115, D24110, doi:10.1029/2010JD014690, 2010b.
Risi, C., Noone, D., Frankenberg, C., and Worden, J.: Role of continental recycling in intraseasonal variations of continental moisture as deduced from model simulations and water vapor isotopic measurements, Water Resour. Res., 49, 4136–4156, 2013.
Rozanski, K.: Deuterium and oxygen-18 in European groundwaters – links to atmospheric circulation in the past, Chem. Geol., 52, 349–363, 1985.
Sachse, D., Radke, J., and Gleixner, G.: Hydrogen isotope ratios of recent lacustrine sedimentary *n*-alkanes record modern climate variability, Geochim. Cosmochim. Ac., 68, 4877–4889, 2004.
Salati, E., Menezes Leal, J., and Mendes Campos, M.: Environmental isotopes used in a hydrogeological study of northeastern Brazil, in: Isotope Techniques in Groundwater Hydrology 1974, Vol. I., International Atomic Energy Agency, Vienna, 379–398, 1974.
Samuels-Crow, K. E., Galewsky, J., Hardy, D. R., Sharp, Z. D., Worden, J., and Braun, C.: Upwind convective influences on the isotopic composition of atmospheric water vapor over the tropical Andes, J. Geophys. Res., 119, 7051–7063, 2014.
Scanlon, B. R., Keese, K., Reedy, R. C., Simunek, J., and Andraski, B. J.: Variations in flow and transport in thick desert vadose zones in response to paleoclimatic forcing (0–

CPD
11, 831–872, 2015

90 kyr): field measurements, modeling, and uncertainties, Water Resour. Res., 39, 1179, doi:10.1029/2002WR001604, 2003.
Schefuß, E., Kuhlmann, H., Mollenhauer, G., Prange, M., and Pätzold, J.: Forcing of wet phases in southeast Africa over the past 17,000 years, Nature, 480, 509–512, 2011.
Schiavo, M. A., Hauser, S., and Povinec, P. P.: Stable isotopes of water as a tool to study groundwater–seawater interactions in coastal south-eastern Sicily, J. Hydrol., 364, 40–49, 2009.
Schlegel, M. E., Mayo, A. L., Nelson, S., Tingey, D., Henderson, R., and Eggett, D.: Paleoclimate of the Boise area, Idaho from the last glacial maximum to the present based on groundwater δ^2H and δ^{18}O compositions, Quaternary Res., 71, 172–180, 2009.
Scholl, M. A., Shanley, J. B., Zegarra, J. P., and Coplen, T. B.: The stable isotope amount effect: new insights from NEXRAD echo tops, Luquillo Mountains, Puerto Rico, Water Resour. Res., 45, W12407, doi:10.1029/2008WR007515, 2009.
Schrag, D. P., Hampt, G., and Murray, D. W.: Pore fluid constraints on the temperature and oxygen isotopic composition of the glacial ocean, Science, 272, 1930–1932, 1996.
Schrag, D. P., Adkins, J. F., McIntyre, K., Alexander, J. L., Hodell, D. A., Charles, C. D., and McManus, J. F.: The oxygen isotopic composition of seawater during the Last Glacial Maximum, Quaternary Sci. Rev., 21, 331–342, 2002.
Shah, A. M., Morrill, C., Gille, E. P., Gross, W. S., Anderson, D. M., Bauer, B. A., Buckner, R., and Hartman, M.: Global speleothem oxygen isotope measurements since the Last Glacial Maximum, Dataset Papers in Geosciences, 2013, 548048, 9 pp., doi:10.7167/2013/548048, 2013.
Shakun, J. D. and Carlson, A. E.: A global perspective on Last Glacial Maximum to Holocene climate change, Quaternary Sci. Rev., 29, 1801–1816, 2010.
Sjostrom, D. J. and Welker, J. M.: The influence of air mass source on the seasonal isotopic composition of precipitation, eastern USA, J. Geochem. Explor., 102, 103–112, 2009.
Stenni, B., Burion, D., Frezzotti, M., et al.: Expression of the bipolar see-saw in Antarctic climate records during the last deglaciation, Nat. Geosci., 4, 46–49, 2011.
Stewart, M. K., Thomas, J. T., Norris, M., and Trompetter, V.: Paleogroundwater in the Moutere gravel aquifers near Nelson, New Zealand, Radiocarbon, 46, 517–529, 2004.
Stute, M. and Deak, J.: Environmental isotope study ^{14}C, ^{13}C, ^{18}O, D, noble gases on deep groundwater circulation systems in Hungary with reference to paleoclimate, Radiocarbon, 31, 902–918, 1989.

CPD
11, 831–872, 2015

Stute, M., Schlosser, P., Clark, J. F., and Broecker, W. S.: Paleotemperatures in the southwestern United States derived from noble gases in ground water, Science, 256, 1000–1003, 1992.

Stute, M., Clark, J. F., Schlosser, P., Broecker, W. S., and Bonani, G.: A 30,000 yr continental paleotemperature record derived from noble gases dissolved in groundwater from the San Juan Basin, New Mexico, Quaternary Res., 43, 209–220, 1995a.

Stute, M., Forster, M., Frischkorn, H., Serejo, A., Clark, J. F., Schlosser, P., Broecker, W. S., and Bonani, G.: Cooling of tropical Brazil (5 °C) during the Last Glacial Maximum, Science, 269, 379–379, 1995b.

Sultan, M., Sturchio, N., Hassan, F. A., Hamdan, M. A. R., Mahmood, A. M., Alfy, Z. E., and Stein, T.: Precipitation source inferred from stable isotopic composition of Pleistocene groundwater and carbonate deposits in the Western desert of Egypt, Quaternary Res., 48, 29–37, 1997.

Tamers, M. A.: Radiocarbon ages of groundwater in an arid zone unconfined aquifer, in: Isotope Techniques in the Hydrologic Cycle, edited by: Stout, G. E., American Geophysical Union Monograph 11, Washington, D.C., 143–152, 1967.

Tan, M.: Circulation effect: response of precipitation δ^{18}O to the ENSO cycle in monsoon regions of China, Clim. Dynam., 42, 1067–1077, 2014.

Tharammal, T., Paul, A., Merkel, U., and Noone, D.: Influence of Last Glacial Maximum boundary conditions on the global water isotope distribution in an atmospheric general circulation model, Clim. Past, 9, 789–809, doi:10.5194/cp-9-789-2013, 2013.

Thatcher, L., Rubin, M., and Brown, G. F.: Dating desert groundwater, Science, 134, 105–106, 1961.

Thompson, L. G., Mosley-Thompson, E., Davis, M. E., Bolzan, J. F., Dai, J., Yao, T., Gundestrup, N., Wu, X., Klein, L., and Xie, Z.: Holocene – late Pleistocene climatic ice core records from Qinghai-Tibetan Plateau, Science, 246, 474–477, 1989.

Thompson, L. G., Mosley-Thompson, E., Davis, M. E., Lin, P. N., Henderson, K. A., Cole-Dai, J., Bolzan, J. F., and Liu, K. B.: Late glacial stage and Holocene tropical ice core records from Huascaran, Peru, Science, 269, 46–50, 1995.

Thompson, L. G., Yao, T., Davis, M. E., Henderson, K. A., Mosley-Thompson, E., Lin, P. N., Beer, J., Synal, H.-A., Cole-Dai, J., and Bolzan, J. F.: Tropical climate instability: the last glacial cycle from a Qinghai-Tibetan ice core, Science, 276, 1821–1825, 1997.

CPD
11, 831–872, 2015

Thompson, L. G., Davis, M. E., Mosley-Thompson, E., Sowers, T. A., Henderson, K. A., Zagorodnov, V. S., Lin, P.-N., Mikhalenko, V. N., Campen, R. K., Bolzan, F. F., Cole-Dai, J., and Francou, B.: A 25,000-year tropical climate history from Bolivian ice cores, Science, 282, 1858–1864, 1998.

Thompson, L. G., Mosley-Thompson, E., Brecher, H., Davis, M., León, B., Les, D., Lin, P.-N., and Mountain, K.: Abrupt tropical climate change: past and present, P. Natl. Acad. Sci. USA, 103, 10536–10543, 2006.

Tierney, J. E., Russell, J. M., Huang, Y., Damsté, J. S. S., Hopmans, E. C., and Cohen, A. S.: Northern Hemisphere controls on tropical southeast African climate during the past 60,000 years, Science, 322, 252–255, 2008.

Tierney, J. E., Smerdon, J. E., Anchukaitis, K. J., and Seager, R.: Multidecadal variability in East African hydroclimate controlled by the Indian Ocean, Nature, 493, 389–392, 2013.

Toscano, M. A., Peltier, W. R., and Drummond, R.: ICE-5G and ICE-6G models of postglacial relative sea-level history applied to the Holocene coral reef record of northeastern St Croix, USVI: investigating the influence of rotational feedback on GIA processes at tropical latitudes, Quaternary Sci. Rev., 30, 3032–3042, 2011.

Ullman, D. J., LeGrande, A. N., Carlson, A. E., Anslow, F. S., and Licciardi, J. M.: Assessing the impact of Laurentide Ice Sheet topography on glacial climate, Clim. Past, 10, 487–507, doi:10.5194/cp-10-487-2014, 2014.

Vimeux, F., Gallaire, R., Bony, S., Hoffmann, G., and Chiang, J. C.: What are the climate controls on δD in precipitation in the Zongo Valley (Bolivia)? Implications for the Illimani ice core interpretation, Earth Planet. Sc. Lett., 240, 205–220, 2005.

Vimeux, F., Tremoy, G., Risi, C., and Gallaire, R.: A strong control of the South American SeeSaw on the intra-seasonal variability of the isotopic composition of precipitation in the Bolivian Andes, Earth Planet. Sc. Lett., 307, 47–58, 2011.

Vuille, M. and Werner, M.: Stable isotopes in precipitation recording South American summer monsoon and ENSO variability: observations and model results, Clim. Dynam., 25, 401–413, 2005.

Wagner, J. D. M., Cole, J. E., Beck, J. W., Patchett, P. J., Henderson, G. M., and Barnett, H. R.: Moisture variability in the southwestern United States linked to abrupt glacial climate change, Nat. Geosci., 3, 110–113, 2010.

Walker, M. J. C., Berkelhammer, M., Björck, S., Cwynar, L. C., Fisher, D. A., Long, A. J., Lowe, J. J., Newnham, R. M., Rasmussen, S. O., and Weiss, H.: Formal subdivision of the

CPD
11, 831–872, 2015

Holocene Series/Epoch: a discussion paper by a working group of INTIMATE (Integration of ice-core, marine and terrestrial records) and the Subcommission on Quaternary Stratigraphy (International Commission on Stratigraphy), J. Quaternary Sci., 27, 649–659, 2012.

Wang, Y. and Jiao, J. J.: Origin of groundwater salinity and hydrogeochemical processes in the confined Quaternary aquifer of the Pearl River Delta, China, J. Hydrol., 438, 112–124, 2012.

Wang, Y. J., Cheng, H., Edwards, R. L., An, Z. S., Wu, J. Y., Shen, C.-C., and Dorale, J. A.: A high-resolution absolute-dated late pleistocene monsoon record from Hulu Cave, China, Science, 294, 2345–2348, 2001.

Werner, M., Mikolajewicz, U., Heimann, M., and Hoffmann, G.: Borehole versus isotope temperatures on Greenland: seasonality does matter, Geophys. Res. Lett., 27, 723–726, 2000.

Werner, M., Langebroek, P. M., Carlsen, T., Herold, M., and Lohmann, G.: Stable water isotopes in the ECHAM5 general circulation model: toward high-resolution isotope modeling on a global scale, J. Geophys. Res., 116, D15109, doi:10.1029/2011JD015681, 2011.

Weyhenmeyer, C. E., Burns, S. J., Waber, H. N., Aeschbach-Hertig, W., Kipfer, R., Loosli, H. H., and Matter, A.: Cool glacial temperatures and changes in moisture source recorded in Oman groundwaters, Science, 287, 842–845, 2000.

Williams, J. W.: Variations in tree cover in North America since the last glacial maximum, Global Planet. Change, 35, 1–23, 2003.

Williams, P. W., Neil, H. L., and Zhao, J. X.: Age frequency distribution and revised stable isotope curves for New Zealand speleothems: palaeoclimatic implications, Int. J. Speleol., 39, 99–112, 2010.

Winnick, M. J., Welker, J. M., and Chamberlain, C. P.: Stable isotopic evidence of El Niño-like atmospheric circulation in the Pliocene western United States, Clim. Past, 9, 903–912, doi:10.5194/cp-9-903-2013, 2013.

Winnick, M. J., Chamberlain, C. P., Caves, J. K., and Welker, J. M.: Quantifying the isotopic "continental effect", Earth Planet. Sc. Lett., 406, 123–133, 2014.

Wolfe, B. B., Edwards, T. W., Aravena, R., Forman, S. L., Warner, B. G., Velichko, A. A., and MacDonald, G. M.: Holocene paleohydrology and paleoclimate at treeline, north-central Russia, inferred from oxygen isotope records in lake sediment cellulose, Quaternary Res., 53, 319–329, 2000.

Wood, W. W., Rizk, Z. S., and Alsharhan, A. S.: Timing of recharge, and the origin, evolution and distribution of solutes in a hyperarid aquifer system, Dev. Water Sci., 50, 295–312, 2003.

CPD
11, 831–872, 2015

Yang, Y., Yuan, D., Cheng, H., Zhang, M., Qin, J., Lin, Y., XiaoYan, Z., and Edwards, R. L.: Precise dating of abrupt shifts in the Asian Monsoon during the last deglaciation based on stalagmite data from Yamen Cave, Guizhou Province, China, Sci. China Ser. D, 53, 633–641, 2010.

Yoshimura, K., Oki, T., Ohte, N., and Kanae, S.: A quantitative analysis of short-term ^{18}O variability with a Rayleigh-type isotope circulation model, J. Geophys. Res., 108, 4647, doi:10.1029/2003JD003477, 2003.

Yoshimura, K., Kanamitsu, M., Noone, D., and Oki, T.: Historical isotope simulation using reanalysis atmospheric data, J. Geophys. Res., 113, D19108, doi:10.1029/2008JD010074, 2008.

Yuan, D., Cheng, H., Edwards, R., Dykoski, C. A., Kelly, M. J., Zhang, M., Qing, J., Lin, Y., Wang, Y., Wu, J., Dorale, J. A., An, Z., and Cai, Y.: Timing, duration, and transitions of the last interglacial Asian monsoon, Science, 23, 575–578, 2004.

Zongyu, C., Jixiang, Q., Jianming, X., Jiaming, X., Hao, Y., and Yunju, N.: Paleoclimatic interpretation of the past 30 ka from isotopic studies of the deep confined aquifer of the North China plain, Appl. Geochem., 18, 997–1009, 2003.

CPD
11, 831–872, 2015

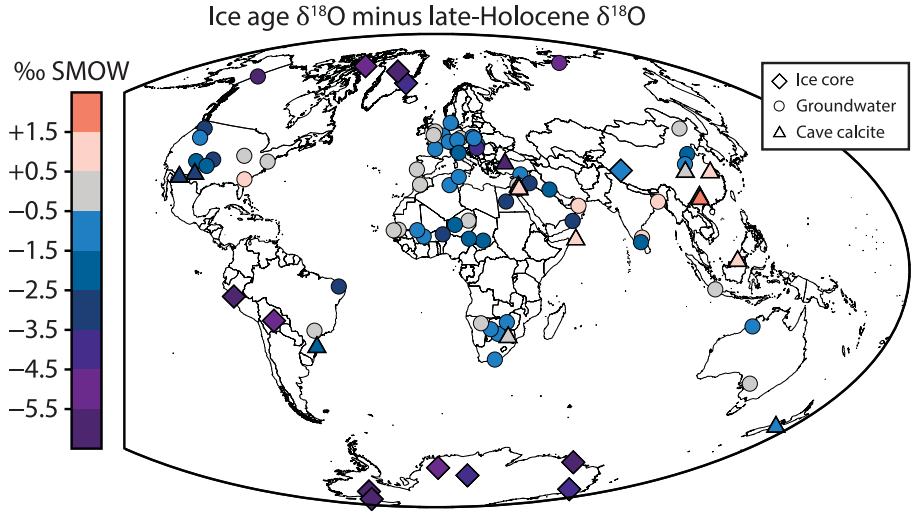

Figure 1. Meteoric water $\delta^{18}O$ change from the latter half of the last ice age (19 500 to ~ 50 000 years ago) to the late-Holocene (within past ~ 5000 years). The low temporal resolution of groundwater records means that $\delta^{18}O$ variations within each time period are smoothed and likely represent unequal temporal weighting. References for reconstructed meteoric water $\delta^{18}O$ changes for ice cores, groundwater and cave calcite are presented in the Supplement.

CPD
11, 831–872, 2015

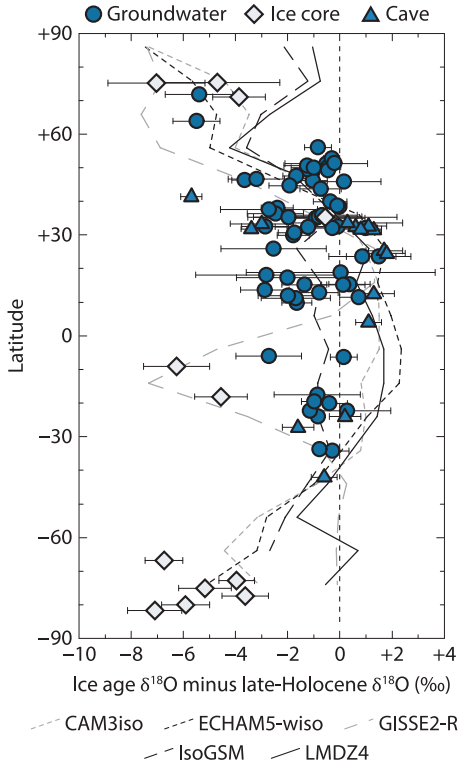

Figure 2. Latitudinal variations of $\Delta^{18}O_{ice\ age}$ values of groundwater (circles, each circle is one aquifer), ice cores (diamonds) and cave calcite (i.e., speleothems; triangles). Dashed lines mark 10° zonal mean simulated $\Delta^{18}O_{ice\ age}$ values from five different general circulation models: CAM3iso, ECHAM5-wiso, GISSE2-R, IsoGSM and LMDZ4 (Yoshimura et al., 2003; Legrande and Schmidt, 2008, 2009; Risi et al., 2010a; Noone and Sturm, 2010; Pausata et al., 2011; Werner et al., 2011).

CPD
11, 831–872, 2015

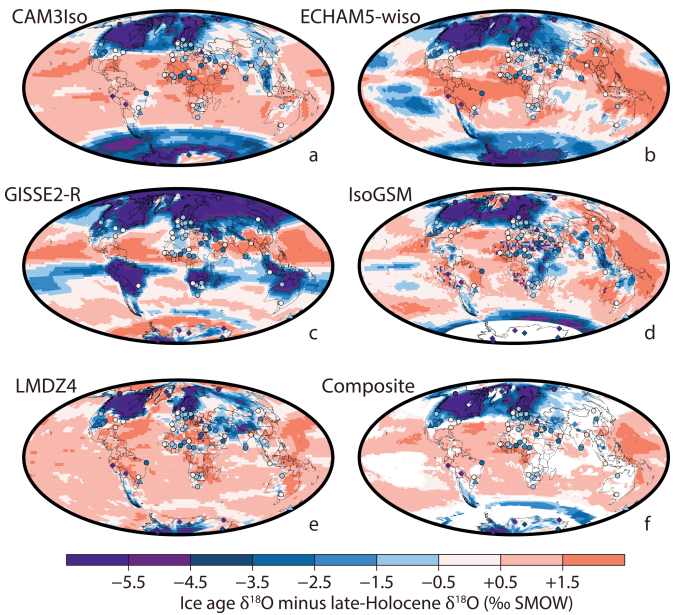

Figure 3. Simulated precipitation $\delta^{18}O$ differences between the last glacial maximum and pre-industrial time periods (i.e., $\delta^{18}O_{\text{last glacial maximum}} - \delta^{18}O_{\text{pre-industrial}}$) from five general circulation models: CAM3iso, ECHAM5-wiso, GISSE2-R, IsoGSM and LMDZ4 (Yoshimura et al., 2003; Legrande and Schmidt, 2008, 2009; Risi et al., 2010a; Noone and Sturm, 2010; Pausata et al., 2011; Werner et al., 2011). Circles (groundwater), triangles (speleothems) and diamonds (ice cores) show reconstructed $\Delta^{18}O_{\text{ice age}}$ values from paleoclimate proxy records (Fig. 1, original data presented in Tables S2–S5). The panel entitled "Composite" shows the multi-model median $\Delta^{18}O_{\text{ice age}}$ value where at least four of the five models agree on the sign of simulated $\Delta^{18}O_{\text{ice age}}$ values (i.e., positive or negative; all five model simulations of $\delta^{18}O_{\text{last glacial maximum}} - \delta^{18}O_{\text{pre-industrial}}$ were used to calculate multi-model median shown in "Composite").

CPD
11, 831–872, 2015